

# $^1\text{H}$ NMR and Calorimetric Measurements on Rabbit Eye Lenses

Aleksander Gutsze<sup>a</sup>, Jerzy Bodurka<sup>a</sup>, Robert Olechnowicz<sup>a</sup>  
Gerd Buntkowsky<sup>b</sup> and Hans-Heinrich Limbach<sup>b</sup>

<sup>a</sup> Department of Biophysics, Medical Academy of Bydgoszcz,  
ul. Jagiellonska 13, 85-067 Bydgoszcz, Poland

<sup>b</sup> Institut für Organische Chemie der Freien Universität Berlin, Takustr. 3,  
D-14195 Berlin, Bundesrepublik Deutschland

Z. Naturforsch. **50c**, 410–418 (1995); received December 19, 1994/February 20, 1995

$^1\text{H}$  NMR, Rabbit Lens, Relaxation Measurements, Line Shape, Water

The dynamic properties of water molecules in the rabbit lens were studied by proton nuclear magnetic resonance line shape analysis, measurements of relaxation times as a function of temperature and calorimetric measurements. The experiments prove, as already suggested by other authors, that there are two types of water in the lens of rabbit eyes, namely bound unfreezable hydration water and bulk freezable water. Line shape analysis and relaxometry showed, that this two types of water exist in two different environments, which may be identified as the nucleus and the cortex of the lens. The line shape analysis showed furthermore that water molecules in the rabbit lens has a common spin lattice relaxation time ( $T_1$ ), but two different transverse relaxation times ( $T_{2A}$  and  $T_{2B}$ ). The tentative model of fast water exchange on the  $T_1$  time scale and slow water exchange on the  $T_2$  time scale, was used to explain experimental proton relaxation data of the rabbit lens. An estimation for this exchange rate  $k_{ex}$  by comparing it to the relaxation times is given ( $T_1^{-1} \ll k_{ex} \ll T_1^{-1}$ ). It has also been shown by a calorimetric measurements, that the lenses can be easily undercooled to temperatures well below the freezing point of water. The achievable maximum undercooling temperature of the lens is a function of the cooling rate  $K_C$ , therefore it has to be considered as an experimentally adjustable parameter which is not characteristic for the investigated sample. Thus it must be noted that any previous discussions about the specific value of the temperature of water crystallisation in biological systems need to be carefully reconsidered.

## Introduction

A rapid progress in the magnetic resonance imaging technique (MRI) has increased the interest in the longitudinal and transverse nuclear magnetic relaxation processes in biological materials. Especially the relaxation properties of water, which may be characterized by a longitudinal or spin-lattice relaxation time  $T_1$  and a transverse or spin-spin relaxation time  $T_2$  play a crucial role (Hutchison, 1985). These values depend in a characteristic way on molecular environment of water molecules, because of different molecular mobility and structures. Thus, the  $T_1$  and  $T_2$  values of the protons of bulk or "freezable" water are much longer than those of water bound to biomolecules. However, because of exchange between these environments only average  $T_1$  and  $T_2$  values are generally observed, which depends on the probabili-

ties of the differed environments. Moreover, water protons can also exchange themselves or the magnetization with mobile protons of external functional OH- or NH-groups of the proteins leading also to contributions of these environments to water relaxation times (Winkler and Michel, 1985; Edzes and Samulski, 1977; Koenig *et al.*, 1978). Nevertheless, these quantities can provide interesting information on changes of protein hydration and mobility, which are themselves related to biological changes (Beall *et al.*, 1984; Bottomley *et al.*, 1984; Hills *et al.*, 1989). Unfortunately, the complexity of biological systems often makes it difficult to elucidate the exact structural changes by NMR-relaxometry. The study of the simplest biological model systems is therefore very important.

A normal mammalian lens contains about 65% of water and 35% of organic material, mainly structural proteins. The main part are crystallins called  $\alpha$ ,  $\beta$  and  $\gamma$  ( $\alpha$  (15%),  $\beta$  (55%), and  $\gamma$  (15%)) which constitute over 85% of the total lens pro-

---

Reprint requests to Dr. J. Bodurka.  
Telefax: (048) 52 22-62-29.

0939-5075/95/0500-0410 \$ 06.00 © 1995 Verlag der Zeitschrift für Naturforschung. All rights reserved.



License: CC BY-NC-ND 3.0 Unported - Creative Commons, Attribution, Non Commercial, No Derivatives

tein. The protein content of the lens (33% of the total weight) is higher than of any other organ in the body (Cotlier, 1981; Slingsby, 1985). A high degree of the physiochemical organisation is needed to get transparency of the lens (Delay and Tardieu, 1983; Bettelheim, 1985). The extent of the total and nonbulk "bound" (non-freezing) water in lenses of various mammals has been established (Cameron *et al.*, 1988; Wang and Bettelheim, 1988). For a rabbit lens the bound water percentage of the total water content is 22% for the cortex and 45% for the nucleus.

The lens exhibits, compared to other tissues, only very low metabolic activities. Measurements of the ATP content on extracted lenses at room temperature have shown (Glonek and Greiner, 1990), that the ATP content does not change on the order of six hours. Thus the extracted lens can survive long outside the organism. This time can be prolonged by further reduction of the metabolic activity of the lens via cooling. Therefore studies of the cooling and water crystallization processes in the lens are of great importance for the storage of lenses, for example for transplantation medicine.

Eye lenses have been studied by NMR-relaxometry in order to elucidate the intrinsic biological differences (Racz *et al.*, 1979; Stankiewicz *et al.*, 1989; Lerman, 1990; Gutsze *et al.*, 1993). During these studies single spin-lattice and two spin-spin relaxation times ( $T_1$ ,  $T_{2A}$ ,  $T_{2B}$  respectively) for the whole lenses have been reported. The origin of this effect is not completely understood yet.

In general, protons in water protein systems may be classified in at least three main phases, according to physico-chemical properties of the environment in which they are located. The proton phases are: proteins, hydration (bound, nonfreezable water, bulk (free) water. Between these phases two exchange processes may exist. First material exchange of proton and molecules (in which protons are located e.g. mainly water molecules). The second exchange process is spin (i.e. magnetization) exchange termed cross-relaxation or, in the case of secular dipolar broadening spin diffusion. It mediates the magnetization transfer particularly in the homonuclear case (Kimmich, 1990; Kimmich *et al.*, 1993).

As water is the main constituent of biological systems, its relaxation behaviour has to reflect re-

laxation behaviour of the lens. The presence of crystallins would be visible by the magnetization transfer between immobilized protein constituents with the hydration water and their change of the dynamic properties (Edzes and Samulski, 1978; Koenig *et al.*, 1993). The common part of all relaxation models in biological systems is an assumption that water molecules exist in at least two different phases (environments), called free (freezable) and bound (nonfreezable) water. Generally, for water proteins solution a fast water molecular exchange between free and bound water environments is assumed. As a result of such assumption a single spin-lattice ( $T_1$ ) and a single spin-spin ( $T_2$ ) relaxation times are expected. Additionally in some systems it were established that the presence of cross-relaxation between protein and water protons may determined the relaxation behaviour. As the result there are observed a non-exponential spin-lattice and spin-spin relaxation functions (Edzes and Samulski, 1978; Bottomley *et al.*, 1984; Koenig *et al.*, 1993).

The lenses exhibit different relaxation behaviour – one records one  $T_1$  and two  $T_2$  values (Stankiewicz *et al.*, 1989; Lerman, 1991; Gutsze *et al.*, 1991). These findings clearly indicate different arrangements and dynamic properties of water molecules in the lens. In order to explain this discrepancy, a tentative simple model of water behaviour in the lens was proposed (Gutsze *et al.*, 1993). According to that in the  $T_1$  time scale (order of seconds) one observed an exchange process which apparent rates in the fast exchange regime, while in the  $T_2$  time scale (order of milliseconds) apparent rate of exchange in the slow exchange regime. In the spin-spin relaxation time for the bound water- $T_{2B}$ , one has to include a cross-relaxation term. Such assumption explains why two  $T_2$  values were observed. Moreover, since chemical shift of free and bound water is expected to be different (Gallier *et al.*, 1988; Kimmich, 1990), the average chemical shift of water in the different compartments should also be different. Thus, one should observe water lines at different positions arising from different compartments.

In the present experimental study further evidence for this model is obtained by a combination of calorimetry, NMR relaxometry and NMR line shape analysis. The latter exploits the different res-

onance frequencies of the mobile protons in the different environments (Kimmich, 1990). The line shape contributions of the various environments show interesting changes with temperature, which help to solve another problem which already arose in the early NMR work on eye lenses. This is the problem of the freezing point of water in the lense, manifesting itself as sudden changes in the relaxation times  $T_1$  and  $T_{2A}$ ,  $T_{2B}$  (Racz *et al.*, 1979; Seiler *et al.*, 1983) could show, that the crystallization temperature of the freezable lens water depends on experimental conditions, while the melting point is almost independent of the latter. Thus, the hysteresis observed for both relaxation times  $T_1$  and  $T_2$  is connected to the effect of undercooling the lens, which was additionally proved by a simple calorimetric method. In the present work the experimental parameters influencing the obtainable undercooling temperature of the lens are elucidated.

### Materials and Methods

Experiments were performed on lenses obtained from five 3-month old rabbits. The temperature measurements of the relaxation times were carried out 1 h post mortem in the temperature range  $294 \pm 233$  K ( $+20^\circ\text{C}$  to  $-40^\circ\text{C}$ ). A pulse NMR-spectrometer (PMS-60, Radiopan Poland) working at 60 MHz was used. The spectrometer was equipped with a temperature control system, which allows stabilization of the probe temperature to the accuracy of 0.5 K. Spin lattice relaxation times were measured by means of the saturation recovery method. The spin-spin relaxation time  $T_2$  was measured by means of Carr-Purcell-Meiboom-Gill (CPMG) method. Only even echoes were registered to reduce effects of the  $B_1$  field inhomogeneity and pulse width errors (Levit and Freeman, 1981). The numerical analysis of the relaxation function was done by a non-linear least squares method (Marquart algorithm (Bevington, 1969)). The line shape of the whole eye lens was measured with a Bruker MSL 300 spectrometer at 293 K and 262 K.

In order to determine the precise undercooling and crystallization temperatures of the lens by an additional method, a simple calorimetric device was designed (Fig. 1), which allows calorimetric measurements of the whole lens and a precise de-

### SIMPLE CALORIMETER

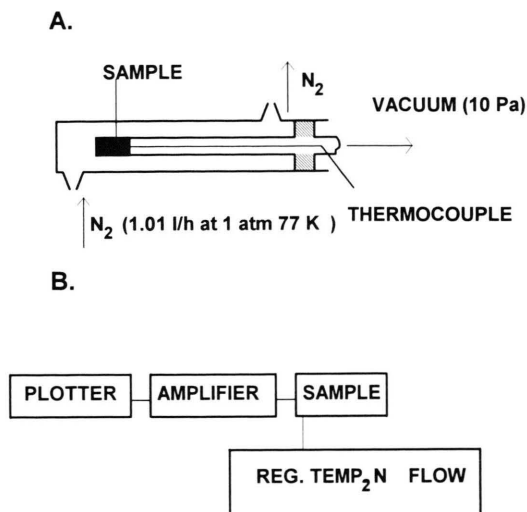


Fig. 1. Simple homemade apparatus (schematically) used for the calorimetry of rabbit eye lenses (A: sample cell, B: block diagram). Gaseous  $\text{N}_2$  flows through a cryostat which contains the sample in an evacuated glass tube. The flow rate of the  $\text{N}_2$  is controlled by changing the boiling rate. The temperature change of the sample is monitored by a thermocouple and registered on a plotter as a function of time.

termination of the crystallization point of the lens as a function of various experimental parameters. In order to measure the undercooling temperature, the lens was placed in a Dewar vessel. The change of temperature was achieved with a constant flux of gaseous nitrogen. The temperature of the lense was measured with a thermocouple and monitored as a function of time during the constant cooling or heating process. The cooling rate  $K_c$  and the heating rate  $K_h$  are experimental parameters expressed as the temperature change of the sample per time unit. These parameters depend on the flux rate of the nitrogen.

### Experimental Results

NMR measurements were performed during cooling/heating cycles between 293 and 233 K. In the whole temperature range the longitudinal relaxation of the whole lens was characterized by a single relaxation time  $T_1$ . Between 293 K and 255 K spin-spin relaxation was bi-exponential, i.e. characterized by two time constants ( $T_{2A}$  and

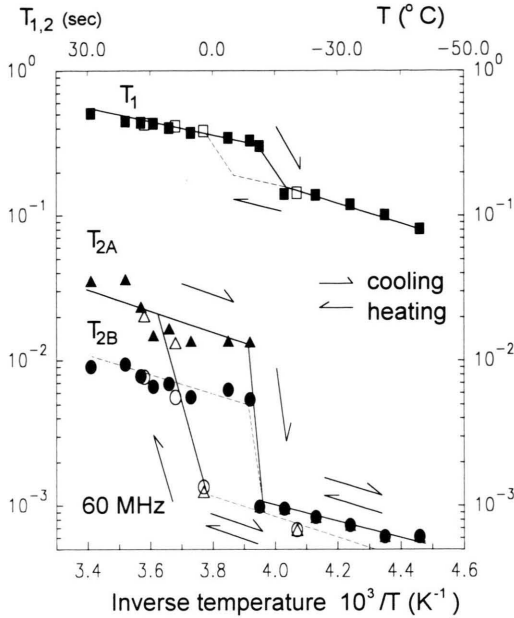


Fig. 2. Results of the <sup>1</sup>H NMR relaxation time measurements performed on an intact rabbit eye lens as a function of temperature in a cooling/heating cycle. Note the hysteresis, caused by undercooling the lens. ■,  $T_1$  cooling; □,  $T_1$  heating; ▲,  $T_{2A}$  cooling; △,  $T_{2A}$  heating; ●,  $T_{2B}$  cooling; ○,  $T_{2B}$  heating.

$T_{2B}$ ). The results are assembled in Fig. 2. At 255 K the main part of the lens water freezes, which shows up in a sudden step of the  $T_{2A}$  and  $T_{2B}$  values. Below the freezing point, the spin-spin relaxation of the frozen water is too fast to be followed in the observed time window ( $T_{2A}$  some microseconds). Therefore only the  $T_{2B}$  decay of the nonfreezable water is observed and the transverse relaxation function appears to be mono-exponential. Note, that water freezing at 255 K also leads to a sudden change in  $T_1$ . The different behaviour of ( $T_1$ ,  $T_{2A}$  and  $T_{2B}$ ) upon cooling and heating (hysteresis) is well manifested in Fig. 2.

The results of a 300 MHz <sup>1</sup>H  $T_1$  experiment performed on a rabbit lens at 293 K, which is well above the freezing point, are shown in Fig. 3. The spectra were obtained by Fourier transforming the FID, which was recorded after the detection pulse for different delay times  $\tau$  in the  $T_1$ -experiment (saturation-recovery sequence). A characteristic pattern is observed at 293 K, exhibiting a relatively sharp intense high field component and a weaker

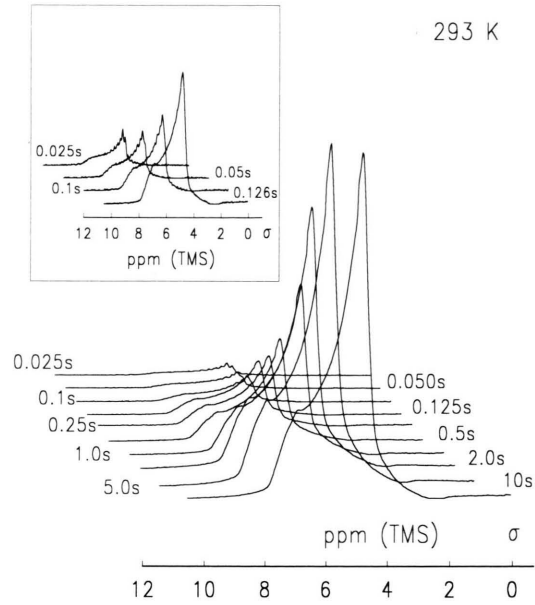


Fig. 3. Spectral resolved  $T_1$  experiment on the lens. Shown is the experimental NMR line shape of the whole rabbit lens at 293 K as a function of the recovery time  $\tau$  between saturation and detection in the saturation recovery sequence. Actual values used for  $\tau$  are : ( $\tau = 10.0, 5.0, 2.0, 1.0, 0.5, 0.25, 0.125, 0.100, 0.050, 0.025$  sec). For better comparison the curves for the short  $\tau$  values are magnified in the insert. Note that the line shape does not depend on  $\tau$ , which suggests, that all spectral components have the same  $T_1$  value.

broader component on the low field side. Although the signal decreases with  $\tau$ , the line shape characteristics remain unchanged, as expected for a frequency independent  $T_1$ .

To support this analysis we performed a numerical line shape analysis of the registered spectra, by deconvoluting them in a sum of  $m$ -Gaussian and  $n$ -Lorentzian lines using the following model function,

$$M(\nu) = \sum_n I_n^L \frac{1}{1 + \left( (\nu - \nu_{0n}) / \beta_n^L \right)^2} + \sum_m I_m^G \frac{1}{1 + \left( (\nu - \nu_{0m}) / \beta_m^G \right)^2} \quad (1)$$

$$\beta_m^G = \frac{1}{2\pi T_{2m}^G}; \quad \beta_n^L = \frac{1}{2\pi T_{2n}^L}$$

where  $I_n^L$ ,  $I_n^G$  are the amplitudes and  $\beta_n^L$ ,  $\beta_n^G$  are the widths of these lines.

The best fit – under the constraint to use a minimum number of lines – was achieved for  $n = 2$  and  $m = 2$ , i.e. for a model function which is a superposition of two Lorentzian and two Gaussian lines (L1, L2, G1, G2). This deconvolution, which matches very well the experimental line shape, is shown in Fig. 4a. For comparison, Fig. 4b shows the best result for  $m = 2$  and  $n = 1$ , which is less satisfactory, because of the strong deviations between experimental and fitted spectrum.

In the next stage, a lineshape analysis of all spectra in Fig. 3 was performed in order to detect the  $T_1$  values of the various signal components.

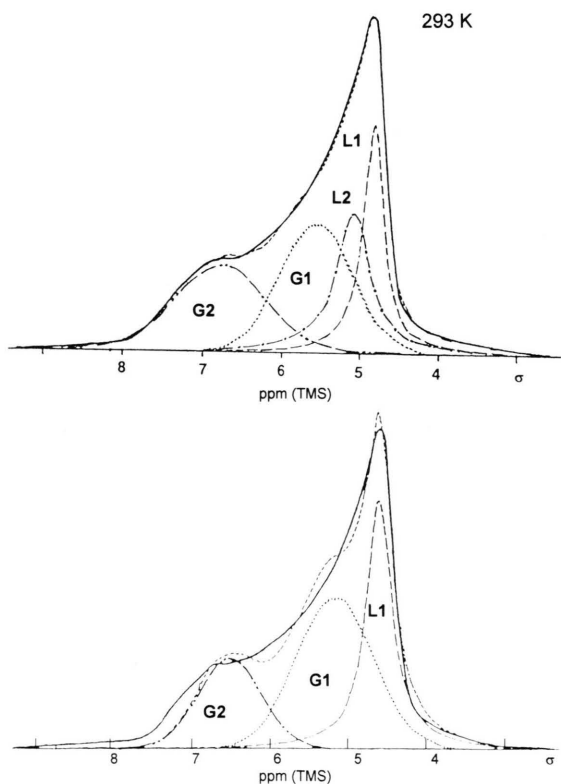


Fig. 4. econvolution of the experimental line shape registered at room temperature (293 K, solid line). Different model functions for reproducing the observed line were used. The upper figure presents the best fit (thin line) obtained for a sum of two Lorentzian (dashed lines, L1, L2) and two Gaussian lines (long dashed, pointed lines, G1, G2). The lower figure shows for comparison the less satisfactory result obtained by fitting the spectrum with the sum of one Lorentzian (thin dashed line, L1) and two Gaussian lines (pointed, solid dashed-pointed lines, G1, G2).

The resulting normalized line intensities ( $I_1^L$ ,  $I_1^G$ ,  $I_2^L$ ,  $I_2^G$ , divided by their asymptotic values for  $\tau \gg T_1$ ) are shown in Fig. 5 as a function of the delay time  $\tau$ . As can be clearly seen, there is only one common spin lattice relaxation time  $T_1$  for the whole system at room temperature.

Interesting line shape changes are observed when cooling the lens down to 255 K, as shown in Fig. 6. The sharp highfield signal has disappeared and the signal now consists of a superposition of a very broad line with a width of 25 kHz and a relative sharp line exhibiting a line width of 2 kHz. We can therefore assume, that the broad line is associated to the sharp highfield signal in Fig. 3, which was decomposed into the Lorentzians (L1, L2), which we now can attribute to the bulk freezable water and the sharp line of Fig. 6 is associated to the non-freezable water (Gaussian lines (G1, G2)).

As already stated, the hysteresis of the relaxation time  $T_1$  and  $T_2$  as a function of the temperature is due to the undercooling of the lens. This

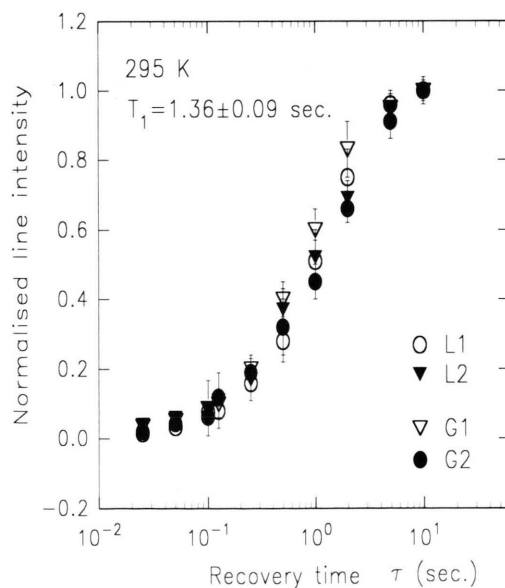


Fig. 5. Result of the spectral deconvolution of the saturation recovery experiment shown in Fig. 3 into the four lines (L1  $\circ$ , L2  $\bullet$ , G1  $\nabla$ , G2  $\blacktriangledown$ ) shown in the upper part of Fig. 4. Shown are the relative intensities of the four lines as a function of the recovery time  $\tau$ . These relative intensities are in very good agreement with each other, which proves, that there is only a single  $T_1$  time of  $1.36 \pm 0.09$  sec at 293 K in the lens.

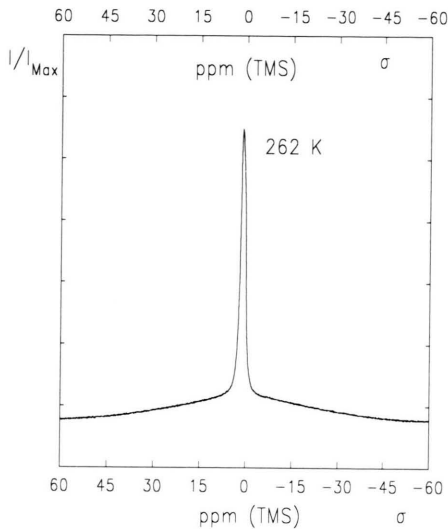


Fig. 6. The NMR line shape of the rabbit lens (same sample as in Fig. 3) registered after partial water freezing at 262 K. The line can be decomposed into a rather narrow component of 6.6 ppm width centered at 5 ppm, which we attribute to the nonfreezable water and a broad component of about 80 ppm caused by the protons from the frozen bulk water and protein protons.

process was also followed by calorimetry using the device described in Fig. 1. The experimental results during a cooling–heating cycle are shown in Fig. 7. It is evident that undercooling of the lens is easy to achieve. After undercooling the lens to a given temperature, a sudden step to higher temperature occurs, caused by the crystallization of the water. After the crystallization is finished the temperature of the lens decreases again. On heating the frozen lens, decrystallization (melting) of the water occurs at 272 K. We found experimentally that this temperature does not depend on the sample or the heating rate  $K_H$ , contrary to the crystallization temperature, which strongly depends on the cooling rates  $K_C$ . This is shown in Fig. 8 where the maximum undercooling (ie. start of crystallization) temperature for different cooling rates  $K_C$  is presented. The inset in Fig. 8 shows, that the maximum undercooling temperature depends approximately linear on the cooling rate in this temperature regime. In other words, the maximum undercooling temperature is an experimental parameter which can be adjusted by the cooling rate and is not characteristic for the state of water in the lens.

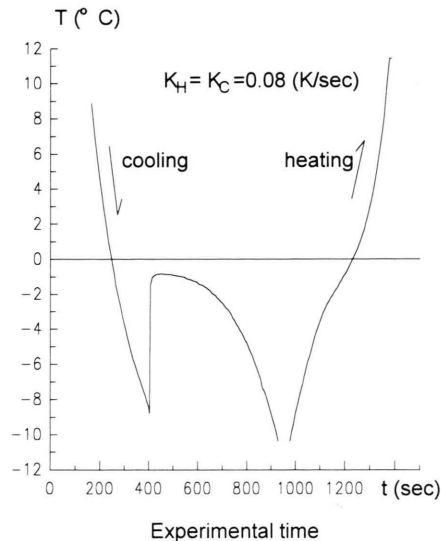


Fig. 7. A typical example of a calorimetric experiment on the rabbit lens. Shown are the temperature changes of the lens during a cooling/heating cycle. The temperature of the lens is registered as a function of the experimental time. Actual cooling and heating rates in the experiment were  $K_C = K_H = 0.08$  K/sec.

## Discussion

As a starting point we want to discuss the origin of the NMR lineshape of the lens shown in (Fig. 3). At a first glance, the shape of the line looks similar to the line observed in solid samples, where unaveraged dipolar interactions among the protons govern the spectrum. These interactions could arise from couplings among protein protons in the crystallins, because these crystallins are relatively immobilized at physiological concentrations (Beaulieu *et al.*, 1988; Morgan *et al.*, 1989). In the literature (Koenig *et al.*, 1993; Belton and Gil, 1993) it has been discussed, that their lineshape is then transferred to both water and protein protons by – compared with  $1/T_1$  – rapid magnetization transfer, which also exists at high fields. Following these ideas a single homogeneous line with complex line shape, characterizable by an exponential longitudinal and, in principle nonexponential spin-spin relaxation functions would be expected. To investigate this mechanism, spectral hole burning experiments (Bloembergen *et al.*, 1948) were performed on the lens (Bodurka, 1995), which have shown that the line is inhomogeneously broadened with a homogeneous line width much smaller than

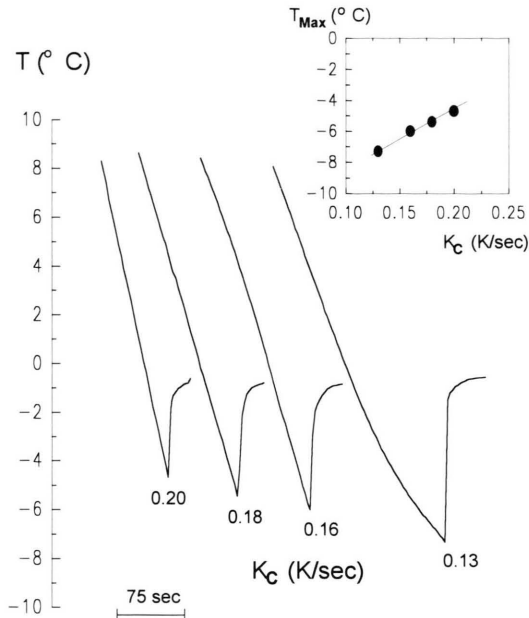


Fig. 8. Results of rabbit eye lens calorimetry for four different cooling rates  $K_C$  of: 0.20, 0.18, 0.16 and 0.13 K/sec. Note the dependence of the maximum undercooling temperature  $T_{\text{Max}}$  on  $K_C$ . The inset on the upper-right side of the figure shows, that this temperature  $T_{\text{Max}}$  depends linearly on the cooling rate  $K_C$ .

the overall width of the lines. Therefore such a mechanism as proposed by (Koenig *et al.*, 1993; Belton and Gil, 1994) can not account for the observed line shape of the rabbit lens.

Therefore the different spectral parts have to be attributed to different types of protons found in the lens and in the following we want to give an interpretation of the experimental spectra in terms of these types of protons. As stated above, we can crudely subdivide the protons into three sub-phases: protein-protons, protons of free water and protons of bound water. Since free water has the highest mobility of these proton phases, it should be associated with the most narrow line observed in the spectrum. Additionally this line should be close to the position of pure water (4.8 ppm TMS). Compared to this we would expect a broader line for the bound water due to the environmental effects of the proteins and the broadest line for the protons directly bound to the proteins. If we compare this to the experimental finding, that the narrow high field component of the spectrum changes to a very broad line during freezing of the lens,

we can clearly attribute this narrow component to the free (freezable) water. The low temperature spectrum, after partial freezing of the water, exhibits a line of about 2 kHz width on top of a broad socket of about 25 kHz. According to the literature typical proton line width of proteins are in the range of 20 kHz (Fyfe, 1983) as well as the proton NMR line width of frozen water (Pfeifer *et al.*, 1976). Therefore we can attribute the 2 kHz line to the hydration (non freezable) water and the broad socket to the protein protons and the frozen water. Thus now we can assign the spectral regions of the high temperature spectrum of Fig. 3 to the three proton phases. The narrow high field line originates from the bulk freezable water, the broader low field component originates from the hydration non freezable water and the protein protons form the socket of the spectrum, ranging over the whole spectral range. In general, effects of the bulk magnetic susceptibility will cause different line positions for water molecules in the nucleus  $v_{1N}$  and the cortex  $v_{1C}$  of the rabbit lens. In the line shape analysis described above, we could show, that the component of the free water is formed by two lorentzian lines and the component of the bound water by two gaussian lines. It is reasonable to attribute these lines to the free water of cortex/nucleus respectively to the bound water of cortex/nucleus.

Regarding the relaxation measurements, we have corroborated in the experiments described above the previous finding (Lerman, 1991; Gutsze *et al.*, 1991) that rabbit eye lenses exhibit a single longitudinal relaxation time  $T_1$  but at least two different transversal relaxation times  $T_{2A}$  and  $T_{2B}$ . We could corroborate the pronounced difference between the  $T_1$  and the  $T_2$ -values, known as the so-called solid like behaviour of water in protein solutions. The presented experimental results allow us already some quantitative discussion in terms of a relaxation model as outlined above. The common  $T_1$  time shows, that on the time scale of  $T_1$  all protons are in the fast exchange regime, i.e. Eqn. (2) is valid. This fast exchange can be caused by chemical exchange between bound and free water, where fast molecular motions of the water molecules average out dipolar interactions among the protons and by cross relaxation between bound water and protein protons. In such a situation for the rabbit lens one can expect to register a

single spin-lattice  $T_1$  and a single spin-spin  $T_2$  relaxation time values given by (Pfeifer, 1972):

$$R_k = \frac{1}{T_v} = \frac{p_A}{T_{vA}} + p_B \left( \frac{1}{T_{vB}} + \frac{1}{T_{vm}} \right);$$

$$v = 1, 2; p_A + p_B \cong 1.0, p_m \ll p_A, p_B \quad (2)$$

where  $p_v$ ,  $1/T_{1v}$   $v = A, B, m$  are the fraction and relaxation rate of water protons in free, bound environments and protein protons respectively.

Furthermore the two different  $T_2$ -values show, that Eqn. (2) is not valid on the time scale of the spin-spin relaxation time. Therefore we can estimate, for the exchange rate of the protons in the eye lense  $k_{ex}$ :

$$T_2^{-1} \ll k_{ex} \ll T_1^{-1}.$$

In further experiments we will analysing the relaxation rates in different parts of the lens and in a subsequent paper we want to discuss these findings in terms of a complete relaxation model of protons in the eye lense.

In summary, we could prove, as already suggested by other authors, that there are two types of water in the lens of rabbit eyes, bound unfreezable hydration water and bulk freezable water. By NMR line shape analysis and relaxometry, we found evidence, that this two types of water exist in two different environments, which may be iden-

tified as the nucleus and the cortex of the lens. The line shape analysis showed furthermore, that all four lines have a common spin lattice relaxation time ( $T_1$ ), but two different transverse relaxation times ( $T_{2A}$  and  $T_{2B}$ ). We could show that the tentative model of fast water exchange on the  $T_1$  time scale and slow water exchange on the  $T_2$  time scale, as proposed (Gutsze *et al.*, 1993) gives a consistent description of the experimental proton relaxation data of the rabbit lens. Furthermore we could give an estimation for this exchange rate by comparing it to the relaxation times. Finally, it has been shown by a calorimetry, that the lenses can be easily supercooled to temperatures well below the freezing point of water and the achievable maximum undercooling temperature of the lens is a function of the cooling rate  $K_C$ . Therefore, the maximum undercooling temperature has to be considered as an experimentally adjustable parameter which is not characteristic for the investigated sample. Thus it must be noted that any previous discussions about the specific value of the temperature of water crystallisation in biological systems need to be carefully reconsidered.

#### Acknowledgements

This work was partly supported by research KBN programme. HHL thanks the Fonds der Chemischen Industrie for financial support.

- Beall P.-T., Amtey S.-R. and Kasturi S.-R. (1984), NMR Data Handbook for Biomedical Applications. Pergamon Press, New York.
- Beaulieu C., Clark C.-L., Brown R.-D., Spiller M. and Koenig S.-H. (1988), Relaxometry of calf lens homogenates, including cross-relaxation by crystallin NH groups. *Magn. Res. Med.* **8**, 45–57.
- Belton P.-S. and Gil A.-M. (1993), Proton NMR line-shapes and transverse relaxation in hydrated barley protein., *J. Chem. Soc. Faraday Trans.* **89**, 4203–4206.
- Bettelheim F.-A. (1985), Physical basis of lens transparency. In: *The Ocular Lens* (H. Maisel, ed). Marcel Dekker Inc., New York, pp. 265–301.
- Bevington P.-R. (1969), *Data Reduction and Error Analysis for Physical Sciences*. McGraw Hill, New York.
- Bloembergen N., Purcell E.-M and Pound R.-V. (1948), Relaxation effects in nuclear magnetic resonance absorption. *Phys. Rev.* **73**, 679–712.
- Bodurka J.-A. (1995), Ph.D. Thesis. Nicholas Copernicus University, Torun, Poland.
- Bottomley P.-A., Foster T.-H., Argersinger R.-E. and Pfeifer L.-M. (1984), A review of normal tissue hydrogen NMR relaxation times and relaxation mechanisms from 1–100 MHz: dependence on tissue type, NMR frequencies, temperature, species, excision, and age. *Med. Phys.* **11**, 425–447.
- Cameron I.-L., Contreras E., Fulerton G.-D., Kellerman M., Ludany A. and Miseta A. (1988), Extent and properties of nonbulk “bound” water in crystalline lens cells. *J. Cell Physiol.* **137**, 125–132.
- Cotlier E. (1981), The lens. In: *Adler’s Physiology of the Eye* (A. Moses, ed.). The C. V. Mosby Company, London, pp. 277–303.
- Delay M. and Tardieu A. (1983), Short range order of crystallin proteins accounts for eye lens transparency. *Nature* **302**, 415–417.

- Edzes H.-T. and Samulski E.-T. (1977), Cross-relaxation and spin diffusion in proton NMR of hydrated collagen. *Nature*. **265**, 259–262.
- Edzes H.-T. and Samulski E.-T. (1978), The measurements of cross-relaxation effects in the proton NMR spin-lattice relaxation of water in biological systems: hydrated collagen and muscle. *J. Magn. Res.* **31**, 207–229.
- Fyfe C.-A. (1983), *Solid State NMR for Chemists*. C. F. C. Press, Guelph, Ontario, Canada.
- Gallier J., Rivet P. and Certaines J. (1987),  $^1\text{H}$  and  $^2\text{H}$  NMR study of bovine serum albumin solutions. *Biochim. Biophys. Acta*. **987**, 1–18.
- Glonek T. and Greiner J.-V. (1990), Intralenticular water interactions with phosphates in the intact crystalline lens. *Ophthalmic Res.* **22**, 302–309.
- Gutsze A., Bodurka J.-A., Olechnowicz R. and Jesmianowicz A. (1993), Nuclear relaxation times in vivo and in vitro of human and rabbit lenses. *Colloids and Surfaces A: Physicochem. and Engineering Aspects* **72**, 295–299.
- Gutsze A., Deninger D., Olechnowicz R. and Bodurka J.-A. (1991), Measurements of proton relaxation time  $T_2$  on cattle eye lenses. *Lens and Eye Tox. Res.* **8**, 155–163.
- Hills B.-P., Takaces S.-F. and Belton P.-S. (1989), The effects of proteins on the proton NMR transverse relaxation times of water. I. Native bovine serum albumin. *Molec. Phys.* **67**, 903–918.
- Hutchison J.-M.-S. (1985), NMR proton imaging. In: *Magnetic Resonance in Medicine and Biology* (M.-A. Foster, ed.). Pergamon Press, Oxford, pp. 157–212.
- Kimmich R. (1990), Dynamic processes in aqueous protein systems. *Molecular theory and NMR relaxation*. *Makromol. Chem., Makromol. Symp.* **34**, 237–248.
- Kimmich R., Nusser W. and Gneiting T. (1990), Molecular theory for nuclear magnetic relaxation in protein solutions and tissues: Surface diffusion and free volume analogy. *Colloids and Surfaces* **45**, 283–302.
- Koenig S.-H., Brown R.-D. and Ugolini R. (1993), A unified view of relaxation in protein solutions and tissue, including hydration and magnetization transfer. *Magn. Res. Med.* **29**, 77–83.
- Koenig S.-H., Bryant R.-G., Hallenga K. and Jacob G.-S. (1978), Magnetic cross-relaxation among protons in protein solutions. *Biochemistry* **17**, 4348–4358.
- Lerman S. (1991), NMR and fluorescence studies on human and animal lenses. *Lens and Eye Tox. Res.* **8**, 121–134.
- Levit M.-H. and Freeman R. (1981), Compensation for pulse imperfections in NMR spin-echo experiments. *J. Magn. Res.* **43**, 65–80.
- Morgan C.-F., Schleich T., Caines G.-H. and Farsworth P. (1989), Elucidation of intermediate (mobile and slow (solidlike) protein motions in bovine lens homogenates by carbon C-13 NMR spectroscopy. *Biochemistry* **28**, 5065–5074.
- Pfeifer H. (1972), NMR and relaxation of molecules adsorbed on solids. In: *NMR Basic Principles and Progress*. Vol. **7**. Springer Verlag, New York, pp. 55–153.
- Pfeifer H., Gutsze A. and Shdanov S.-P. (1976), State of water in fujasite-type zeolites. Part I, higher loading. Part II, lower loading. *Z. Phys. Chem. (Leipzig)* **257**, 721–734.
- Racz P., Tompa K. and Pocsik I. (1979), The state of water in normal human, bird and fish lenses. *Exp. Eye Res.* **29**, 601–608.
- Seiler T., Muller-Stolzenberg N. and Wollensak J. (1983), Phase transitions in ocular tissue NMR and temperature measurements. *Graefes Arch. Exp. Ophthalmol.* **221**, 122–125.
- Slingsby C. (1985), Structural variation in lens crystallins. *Trends Biochem. Sci.* **10**, 281–294.
- Stankiewicz P.-J., Metz K.-R., Sassani J.-W. and Briggs R.-W. (1989), Nuclear magnetic resonance study of free and bound water fractions in normal lenses. *Invest. Ophthalmol. Vision Sci.* **30**, 2361–2369.
- Wang X. and Bettelheim F.-A. (1988), Distribution of total and non-freezable water contents of galactosemic rat lenses. *Current Eye Res.* **7**, 771–776.
- Winkler H. and Michel D. (1985), Exchange processes in NMR. *Adv. in Coll. and Interf. Sci.* **23**, 149–179.